Post processing of ozone data measured during BBFlux aircraft campaign (July – September 2018)

Andreas Zahn and Florian Obersteiner (andreas.zahn@kit.edu; f.obersteiner@kit.edu)

O_3 mixing ratio underestimation

Instrument intercomparisons during the campaign (flight 25 of 39) and after the campaign (at ground) showed a significant underestimation of ozone mixing ratios by the KIT O_3 instrument "FAIRO-4" (FAIRO: Fast AIRborne Ozone instrument). The problem was not present during its calibration prior to the campaign at KIT and never occurred during the 15 years along which FAIROs are in use.

FAIRO combines two ozone sensors: a) a dual-channel UV-photometer (UV-P, time resolution: 0.25 Hz) and a dry chemiluminescence detector (CI-D, time resolution: 12.5 Hz). The CI-D data is calibrated using the UV-P data in post-processing; see [Zahn et al., AMT, 2012].

Underestimation: origin

The UV-P measures the absorption of light by ozone within the Hartley band around 255 nm:

$$I = I_0 \cdot e^{-\sigma(\lambda) \cdot l \cdot n \cdot O3} \qquad (1)$$

with $\sigma(\lambda)$ absorption cross section at λ ~ 255 nm
l absorption length (~38 cm)
n concentration of air molecules
O_3 O_3 mixing ratio

A simple modification leads to

$$O_3 = \mathrm{const}(T, p) \cdot \ln(I/I_0) \qquad (2)$$

That is, each UV-P in principle needs reference measurements of zero-ozone air (no UV absorption) to reference the detector signal (zero-absorption-intensity; I_0). To generate zero-ozone air, an ozone scrubber being a Hopcalite (MnO_2/CuO) catalyst is used in most UV-P ozone instruments including FAIRO. Before shipment of FAIRO-4 to the US, the scrubber did its job and calibrations worked as expected.

Tests done at KIT after the campaign however revealed that the scrubber in FAIRO-4 did not destroy 100% of the ozone, i.e., provided a wrong reference signal I_0. In this case, each ozone absorption measurement (intensity I) is referenced against a false zero-measurement I_0. Ozone mixing ratio calculated from the ratio I/I_0 is therefore too low. This malfunction explains the apparently too low O_3 mixing ratios observed. The tests done at KIT in March 2019 were to quantify the scrubber efficiency, depending on time, ozone mixing ratio and sample flow rate.

Correction Scheme

To correct the BBFlux ozone data, a post-processing scheme is developed. The idea is to model the (time-dependent) scrubber efficiency $E_{scr}(t)$ based on which the correct O_3 data can be inferred:

$$O_3 = O_{3,raw} / E_{scr} \qquad (E_{scr} = 0 \ldots 1)$$

The experiments in March 2019 revealed the following properties of the scrubber in FAIRO-4:

1. E_{scr} degraded over time when exposed to ozone and moisture:
   - while being 100% at first, over multiple experiments done on subsequent days, E_{scr} degraded continuously
   - the scrubber partially recovered between subsequent experiments, that is, E_{scr} was always higher at the beginning of an experiment than at the end of the preceding experiment
2. E_{scr} is flow-dependent:
   - while the fresh catalyst shows nearly 100% efficiency at a flow up to 5 L/min, E_{scr} of the aged scrubber significantly decreases with flow
3. There is also a very weak negative correlation of E_{scr} with ozone. That is, at high ozone levels some more ozone molecules survive the transit through the scrubber.

Constraints

Based on the initial calibration at KIT (May 2018) and the comparison against the Thermo instrument after the campaign (still in the US), E_{scr} approximately falls within the following boundaries:

	Campaign Start	**Campaign End**
Flight Start	1.0	0.9
Flight End	1.0	0.6

Estimation of E_{scr}

For characterising the efficiency of the scrubber E_{SCR} (1: 100%, 0: no scrubber effect), it was dismounted of FAIRO-4 and put between an ozone generator and a reference instrument:

a) To quantify degradation of the scrubber E_{degr} at constant flow rate on the short-term during single experiments (comparable to a campaign flight) and on the long-term from repeated experiments
b) To quantify the flow dependency E_{flow} by varying the flow rate (during short time periods wherein degradation over time is negligible), again during repeated experiments
c) To quantify the dependency on the ozone mixing ratio by varying the generated ozone mixing ratio at constant flow rate (during short time periods wherein degradation over time is negligible)

E_{scr} over the course of the campaign is then calculated as

$$E_{scr} = E_{degr} * E_{flow}$$

Parametrisations of the individual parameters are given in Appendix: Parametrisations.

Ozone mixing ratio dependency (item c) was found to be very small (0.0003 ppb/ppb) and therefore neglected. The scrubber efficiency E_{scr} inferred for the entire BBFlux campaign is shown in Figure 1. The corrected ozone mixing ratio can then be calculated as $O_{3,\,postproc}(t) = O_{3,\,raw}(t)/E_{scr}(t)$.

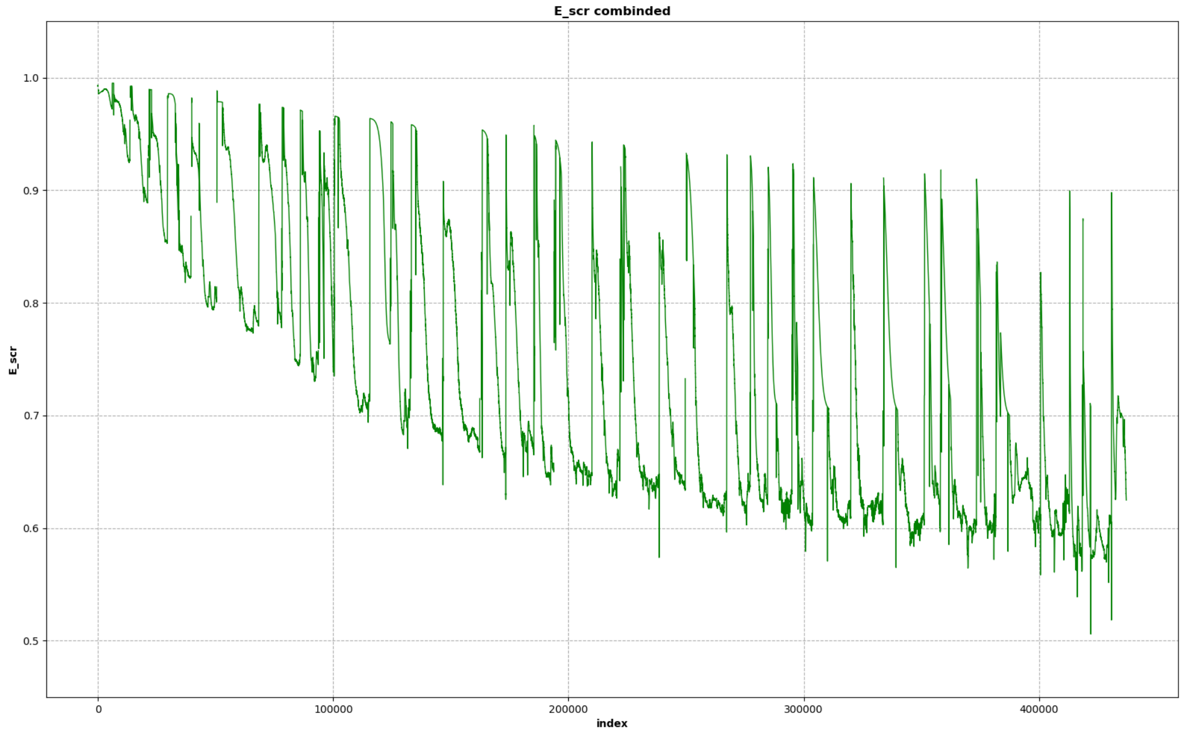

Figure 1. Modelled scrubber efficiency E_{scr} for the BBFlux campaign, displayed as a function of vector index (equal to cumulative seconds of instrument on-time).

As prescribed, the scrubber efficiency degrades over the campaign, from nearly 100% at the beginning to 90% at the end. During each flight (on-phase of the instrument), additional short-term degradation takes place, with a minimum of 60% at the end of the campaign. The observable variability on the very short time scale is caused by the flow component E_{flow}.

Fehler! Verweisquelle konnte nicht gefunden werden. shows an overview of the resulting changes in mean mixing ratio measured during each flight.

Table 1. Absolute and relative change of mean O_3 mixing ratio for all flights.
Relative change = ($O_{3,\ postproc}$ – $O_{3,\ raw}$)/$O_{3,\ raw}$ = 1/E_{scr} – 1.

Flight	absolute change [ppb]	relative change (%)
RF01	2.0	4.2%
RF02	3.3	7.0%
RF03	5.1	10.3%
RF04	10.4	19.9%
RF05	10.9	22.2%
RF06	9.1	20.3%
RF07	7.4	16.4%
RF08	8.8	23.1%
RF09	9.3	25.3%
RF10	5.7	14.9%
RF11	11.3	30.7%
RF12	5.4	14.6%
RF13	14.3	35.4%
RF16	14.7	34.4%
RF17	15.9	36.9%
RF18	20.5	45.4%
RF19	18.7	45.5%
RF20	18.7	43.8%
RF21	14.6	43.2%
RF22	13.8	40.0%
RF23	19.6	57.2%
RF24	11.8	48.9%
RF25	15.8	51.9%
RF26	16.6	58.9%
RF27	18.8	61.6%
RF28	19.7	60.6%
RF29	15.4	50.0%
RF30	14.7	62.2%
RF31	14.5	55.4%
RF32	15.1	64.0%
RF33	14.8	62.4%
RF34	15.9	58.1%
RF35	18.8	61.0%
RF37	15.4	70.8%
RF38	19.0	69.8%
RF39	19.1	44.8%

Updated ozone data: In-flight intercomparison RF25

The following Figure 2 to Figure 5 show a comparison of the FAIRO data against the NCAR ozone instrument on board the C-130 aircraft.

Prior to post-processing

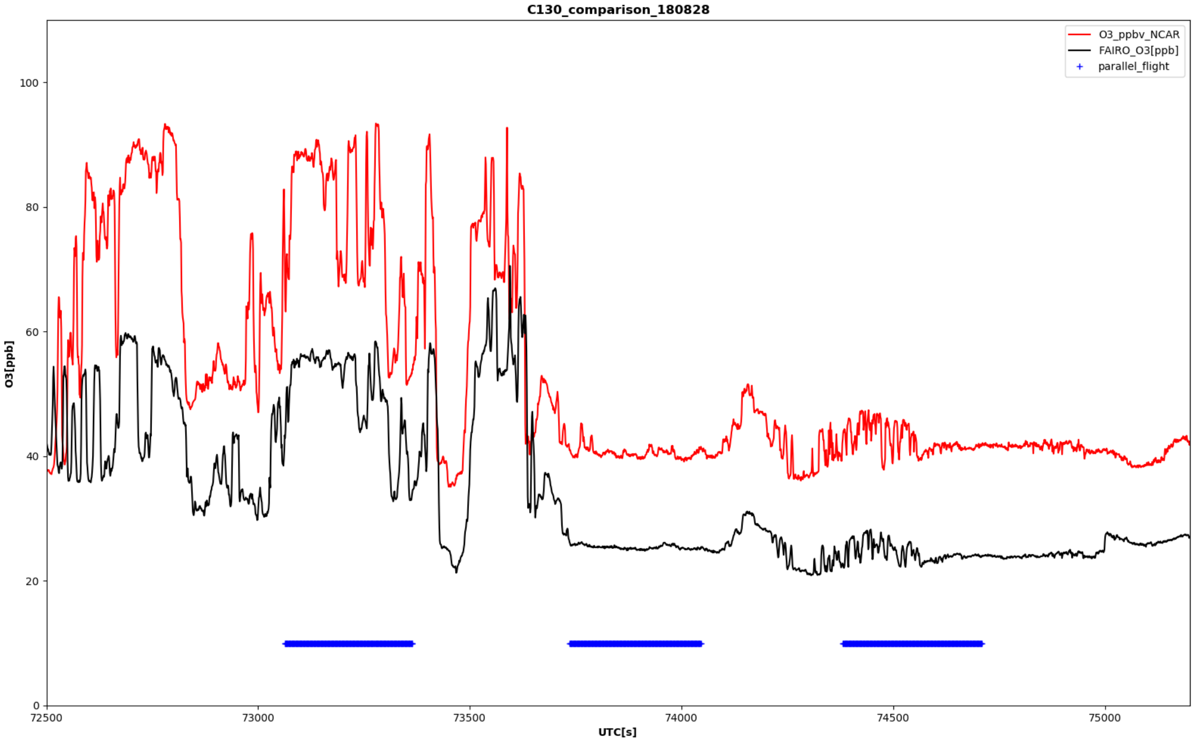

Figure 2. Comparison of absolute ozone mixing ratios for RF25 before post-processing. Red: NCAR instrument (reference) on board the C-130, black: FAIRO-4 on board the KingAir, blue markers: sections of parallel flight (C-130 and KingAir).

There is a pronounced variability of atmospheric ozone observed by both instruments; especially during the first and third section of parallel flight. Obviously, there is a systematic bias between the instruments; the values indicated by FAIRO are too low by on average ~38% (Figure 3).

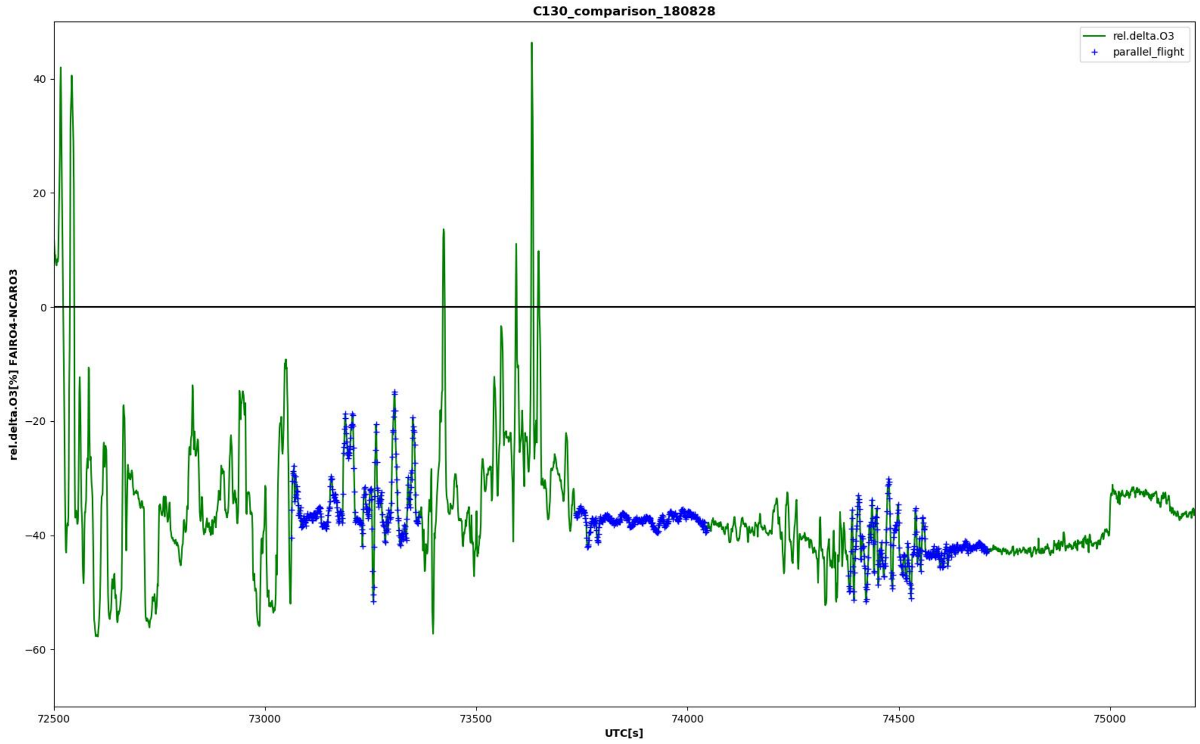

Figure 3. Relative difference between NCAR and FAIRO instrument, calculated as (O3_FAIRO-O3_NCAR)/O3_NCAR) before post-processing. Green: relative deviation of measured ozone mixing ratios, blue markers: sections of parallel flight. Averages of the relative deviations within the parallel flight sections (from left to right): I: -34.0%, II: -37.3%, III: -42.4%.

After post-processing

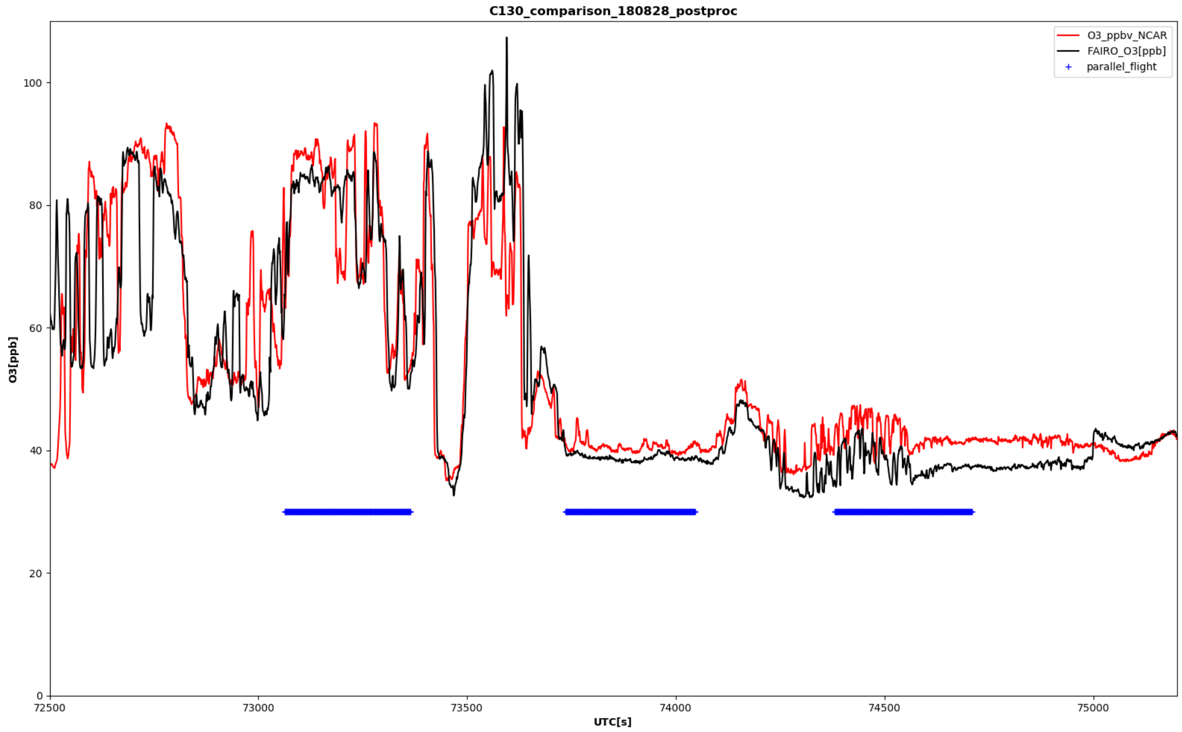

Figure 4. Comparison of absolute ozone mixing ratios for RF25 after post-processing. Red: NCAR instrument (reference) on board the C-130, black: FAIRO-4 on board the KingAir, blue markers: sections of parallel flight (C-130 and KingAir).

After post-processing, observations by both instruments are in much better agreement. The average deviation of FAIRO relative to NCAR is now ~-5%, see Figure 5.

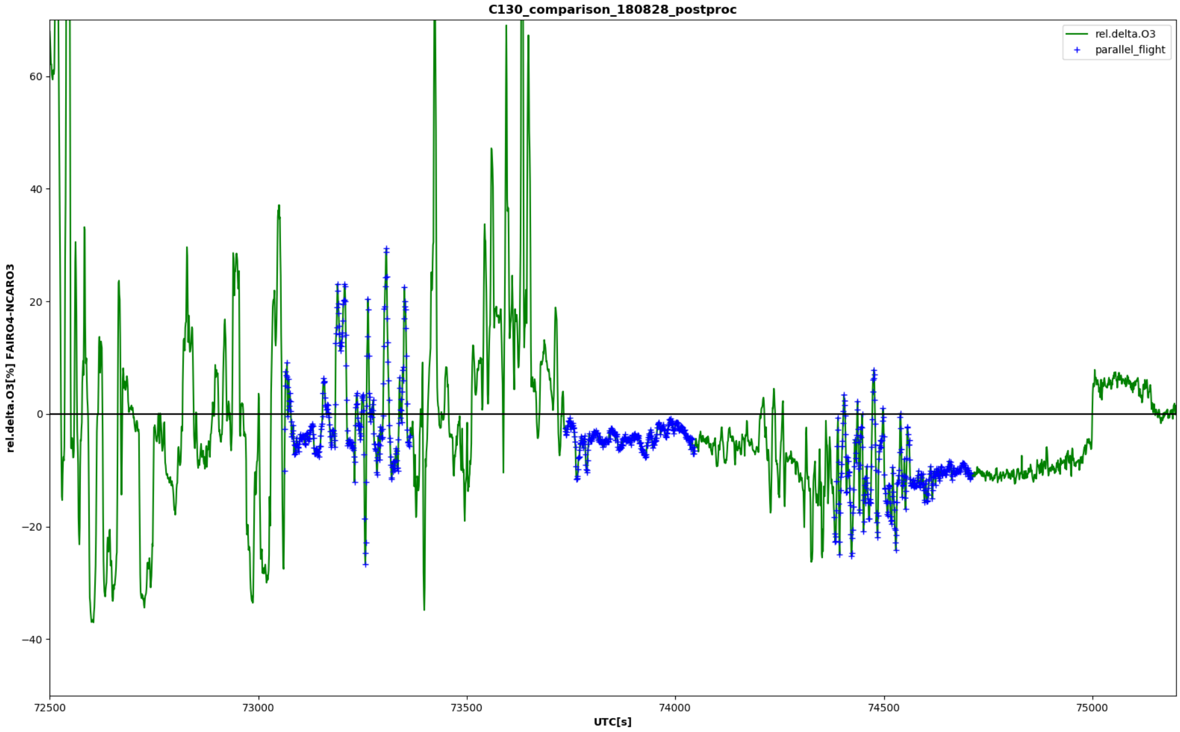

Figure 5. Relative difference between NCAR and FAIRO instrument, calculated as (O3_FAIRO-O3_NCAR)/O3_NCAR) after post-processing. Green: relative deviation of measured ozone mixing ratios, blue markers: sections of parallel flight. Averages of the relative deviations within the parallel flight sections (from left to right): I: 0.0%, II: -4.2%, III: -10.8%.

As indicated on Figure 5, accuracy of post-processed results is significantly improved. However, there is likely still a slight negative bias of up to 10%.

Appendix: Parametrisations

Time vector

Instrument on time, i.e. in state “measure” (MS).

Scrubber degradation over the campaign: E_{min} and E_{max} at the beginning of a flight

$E_{min}(t) = a*exp(-b*t) + c$

with t being time in total seconds of instrument operation and
parameters a, b, c: 0.35, 0.000007, 0.65

$E_{max}(t)$ is assumed to be 1 at the beginning of the campaign and decreasing linearly with operation time to 0.9 at the end of the campaign.

Scrubber degradation during a flight

$E_{degr}(t) = 1 - (1/(1 + exp(-a*(t-b))))$

with t being the time in total seconds of instrument operation since turn-on for the specific operation phase (e.g. a flight), a = 0.001 (constant) and
b being a “delay parameter” before degradation becomes significant in this context. b is varied linearly over the campaign;

Beginning (“new scrubber”): b = 10000

End (“degraded scrubber”): b = 0

$E_{degr}(t)$ is furthermore constrained to give an output within the boundaries E_{min} and E_{max}:

$E(flight) = E(flight) *(E_{max} - E_{min})/(max(E(flight)) - min(E(flight))) + E_{min}$

And if $E(flight)[t] > E_{max}$

$E(flight) = E(flight) - (E(flight)[t=0] - E_{max})$

Scrubber regeneration after a flight

Regeneration is assumed to follow

$E_{reg}(t) = at^3+bt^2+ct+d$

with a, b, c, d = 6.019E-14, -7.986E-10, 7.653E-06, 5.995E-01

Flow dependency

$E_{flow}(flow) = a * log(flow) + b$

with flow being the half mass flow [L/min] calculated from the volume flow measured by the instrument’s internal flow meter as well as inlet pressure and temperature.

Parameters a and b are varied over the campaign as follows:

Beginning (“new scrubber”): -0.050, 1.0300
Middle (“medium degraded scrubber”): -0.287, 1.1989
End (“degraded scrubber”): -0.350, 1.2426